

## Positive exchange bias and upward magnetic relaxation in a Fe-film/CoO-nanoparticle hybrid system

Wei Zhang, Tianlong Wen, and Kannan M. Krishnan

Citation: *Appl. Phys. Lett.* **101**, 132401 (2012); doi: 10.1063/1.4754610

View online: <http://dx.doi.org/10.1063/1.4754610>

View Table of Contents: <http://apl.aip.org/resource/1/APPLAB/v101/i13>

Published by the [American Institute of Physics](http://www.aip.org).

### Related Articles

Enhanced inverse spin-Hall effect in ultrathin ferromagnetic/normal metal bilayers

*Appl. Phys. Lett.* **102**, 072401 (2013)

Heat-induced damping modification in yttrium iron garnet/platinum hetero-structures

*Appl. Phys. Lett.* **102**, 062417 (2013)

Effect of antiferromagnetic thickness on thermal stability of static and dynamic magnetization of NiFe/FeMn multilayers

*J. Appl. Phys.* **113**, 063913 (2013)

Crystal structure of Co/Cu multilayers prepared by pulse potential electrodeposition with precisely controlled ultrathin layer thickness

*AIP Advances* **3**, 022119 (2013)

Anomalous Hall effect and magnetoresistance behavior in Co/Pd<sub>1-x</sub>Ag<sub>x</sub> multilayers

*Appl. Phys. Lett.* **102**, 062413 (2013)

### Additional information on *Appl. Phys. Lett.*

Journal Homepage: <http://apl.aip.org/>

Journal Information: [http://apl.aip.org/about/about\\_the\\_journal](http://apl.aip.org/about/about_the_journal)

Top downloads: [http://apl.aip.org/features/most\\_downloaded](http://apl.aip.org/features/most_downloaded)

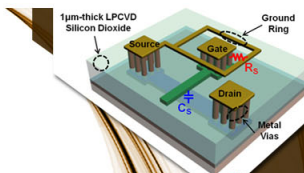
Information for Authors: <http://apl.aip.org/authors>

## ADVERTISEMENT



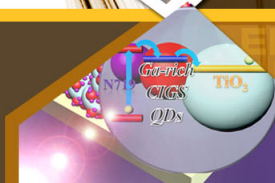
EXPLORE WHAT'S  
NEW IN APL

SUBMIT YOUR PAPER NOW!



### SURFACES AND INTERFACES

Focusing on physical, chemical, biological, structural, optical, magnetic and electrical properties of surfaces and interfaces, and more...



### ENERGY CONVERSION AND STORAGE

Focusing on all aspects of static and dynamic energy conversion, energy storage, photovoltaics, solar fuels, batteries, capacitors, thermoelectrics, and more...

## Positive exchange bias and upward magnetic relaxation in a Fe-film/CoO-nanoparticle hybrid system

Wei Zhang, Tianlong Wen,<sup>a)</sup> and Kannan M. Krishnan<sup>b)</sup>

Department of Materials Science and Engineering, University of Washington, Seattle, Washington 98195, USA

(Received 31 July 2012; accepted 7 September 2012; published online 24 September 2012)

Unusual positive exchange bias found in Fe/CoO<sub>x</sub> nanoparticle bilayer films is correlated to a characteristic magnetic spin-glass (SG) in CoO<sub>x</sub>, with the SG magnetization coupled antiparallel with the Fe magnetization upon field cooling. This SG magnetization has strong field- and time-dependence which displays unusual upward magnetic relaxation behavior in thermoremanent magnetization measurements. The antiparallel coupling is shown to result predominantly from the antiferromagnetic superexchange of the Fe<sup>2+</sup>-O-Co<sup>3+</sup> couple, of the oxygen-terminated CoO<sub>x</sub> at the interface. These experimental results reveal the possibility of manipulating the exchange bias effect via an indirect exchange coupling mechanism. © 2012 American Institute of Physics. [<http://dx.doi.org/10.1063/1.4754610>]

The exchange-bias (EB) effect<sup>1</sup> is central to the design and operation of practical spin electronics devices such as spin valves and magnetic tunnel junctions. Despite these applications, comprehensive understanding of EB has been elusive and remains a long-standing problem involving fundamental questions of surface and interface magnetism.<sup>2</sup> Phenomenologically, the EB effect manifests itself as a shift of the hysteresis loop along the field axis due to a unidirectional interface exchange coupling of a ferromagnet (FM) and an antiferromagnet (AF). Typically, this shift of the hysteresis loop is in the negative field direction when cooled in a positive magnetic field and is usually referred to as negative EB. Such FM/AF coupling has been widely studied in thin-film samples<sup>2</sup> in which the FM and AF phases, including their crystallography<sup>3</sup> and interface spin-lattices,<sup>4</sup> can be well-defined by controlling deposition conditions and studied with electrons and photons.<sup>5</sup> Recently, works on polycrystalline EB samples also showed that the AF layer is made of exchange-decoupled grains, whose size and size distribution play key roles to the EB effect. These AF grains, ~10 nm in size, essentially resemble small nanoparticles (NPs).<sup>6</sup> Therefore, hybrid EB bilayers with the AF layer being chemically synthesized NPs may bring pathways for tailoring their EB properties due to their controllable size, size distribution, morphology, and crystallinity.<sup>7</sup> Such hybrid systems have not been reported so far. In addition, in nanostructured samples,<sup>8</sup> such as NPs,<sup>9,10</sup> a spin-glass (SG) state can be experimentally observed, particularly in metal-oxides<sup>11,12</sup> and -carbides,<sup>13</sup> that show antiferromagnetic (AF) correlations. Such a SG state arises from the random configuration of the surface magnetic moments and uncompensated surface spins with particularly enhanced contributions in NPs due to their large surface-to-volume ratio.<sup>14</sup> Further, such SG phases give rise to exotic properties when coupled with FM phases. Recently, experiments on FM/SG

coupled bilayers showed EB related effects<sup>15</sup> that are typically observed in FM/AF coupling. In particular, unusual positive EB, in addition to the conventional negative EB,<sup>12,16</sup> has been discovered in the FM/SG system and tentatively interpreted by an effective antiparallel coupling across the FM/SG interface.<sup>17</sup> Further, temperature dependent measurements revealed subsequent decay of the positive EB after its establishment around blocking temperature, indicating that it may be a metastable state.<sup>18–20</sup> The disorder of the small AF grains or the grain boundaries have tentatively accounted for the above experimental observations. However, particularly lacking in these models for such positive EB and the antiparallel coupling at the interface is a viable physical explanation for the origins of this phenomenon. Hybrid systems with the AF grains being replaced by NPs may provide a better route for revealing the important role of the AF grains to the EB effect.

In this letter, we describe the discovery and investigation of a positive EB effect in a Fe-film/CoO<sub>x</sub>-NP hybrid system. We reveal the co-existence of a positive EB with a SG magnetization,  $M_{SG}$ , which exhibit a strong relaxation effect depending on the magnetic cooling field and temperature. This SG magnetization is coupled antiparallel to the FM magnetization upon field-cooling, as revealed by an *increase* in the field-free magnetization with time, i.e., a unique *upward* magnetization relaxation. This antiparallel coupling is further attributed to the antiferromagnetic superexchange interactions<sup>21</sup> of the local Fe-O-Co couples at the interface. Temperature dependent measurements show that the EB is determined by competing superexchange and conventional direct exchange interactions. Finally, our experimental results reveal the possibility of manipulating the EB effect via such an indirect exchange-coupling mechanism.

Bilayer samples were fabricated as follows: Co NPs (10 nm in diameter and with a narrow size distribution) were chemically synthesized by a thermal decomposition method.<sup>7,22,23</sup> Co-NP films, a few layers thick, were obtained by assembling these chemically synthesized Co NPs on clean Si substrates via a controlled solvent evaporation technique.<sup>24</sup> The films were annealed at 400 °C in a continuous

<sup>a)</sup>Present address: Department of Physics, Carnegie Mellon University, Pittsburgh, Pennsylvania 15213, USA.

<sup>b)</sup>Author to whom correspondence should be addressed. Electronic mail: kannanmk@uw.edu.

O<sub>2</sub> flow furnace for 1.5 h to convert the Co NPs to Co-oxide NPs. Consistent with the O-rich annealing conditions, *x*-ray photoelectron spectroscopy (XPS)<sup>25</sup> confirmed that the surface of CoO<sub>x</sub> is predominantly the thermodynamically stable Co<sub>3</sub>O<sub>4</sub> with a CoO minor phase. Scanning electron microscopy, Fig. 1(a), showed the particle size  $\sim 10$  nm diameter and atomic force microscopy (AFM), Fig. 1(b), confirmed a surface roughness  $< 4$  nm. Next, we deposited a 30 nm Fe film followed by a 5 nm Ta cap, by ion beam sputtering at a base pressure  $\sim 1 \times 10^{-7}$  Torr on top of the Co-oxide NP film. The magnetic properties were measured by a Quantum Design physical property measurement system over a wide range of temperatures and applied fields.

Hysteresis loops of the sample at various temperatures from 10 to 300 K were measured (Fig. 1(c)) and the temperature dependence of the coercivity,  $H_c$ , and the bias field,  $H_{eb}$ , are summarized in Fig. 1(d). The sample was initially cooled under a magnetic field,  $H_{cool} = 10$  kOe from 380 K down to 10 K and then measured on increasing temperature. For all  $T < 200$  K, the hysteresis loops exhibit a negative shift from the origin which is a signature of conventional EB. This EB is attributed to the exchange coupling between Fe and ordered CoO, below the blocking temperature ( $T_B, \sim 186$  K) of the antiferromagnetic CoO phase.<sup>18</sup> When the sample is measured at temperatures higher than 200 K (CoO disordered), the loop-shift has switched to the same direction as  $H_{cool}$ , which indicates an unconventional positive EB and its magnitude,  $H_{eb} \sim 9$  Oe, remains roughly unchanged from 200 to 300 K. Careful calibrations and repeated measurements were performed to ensure that the measured EB effect came from the sample and not the magnetometer.

The change in sign of EB points directly to a change in the nature of the *effective coupling* across the Fe/Co-oxide

interface. As illustrated in Fig. 2(a), below 200 K, the CoO AF phase is well established thus the effective parallel ( $J_1 > 0$ ) coupling between Fe ( $S_{Fe}$ ) and Co ( $S_{Co}$ ) spins, gives rise to the conventional negative EB.<sup>18</sup> At above 200 K when the CoO loses its magnetic order, the result of the effective antiparallel coupling ( $J_2 < 0$ ) between  $S_{Fe}$  and the local SG magnetizations becomes visible (the origin of such coupling will be discussed later). To gain more insight into the physical mechanism of such coupling, we performed detailed field- and time-dependent measurements. Samples were initially cooled from 380 K to 300 K under various positive cooling fields,  $H_{cool}$ ; after the temperature stabilized at 300 K, the hysteresis loops were measured (Fig. 2(b)). Rounded hysteresis loops, rather than squared ones, were observed due to the imperfect Fe crystallinity of the particle film. Positive EB was observed and its value slightly increases with increasing  $H_{cool}$  ( $= 0.5, 1, 2, 3, 5, 10$  kOe). We then switched  $H_{cool}$  to negative fields and negative EB were observed as expected (not shown here). We then measured hysteresis loops after 24 h and found the EB disappeared, regardless of the *magnitude* or *direction* of  $H_{cool}$  (Fig. 2(b)). It also reconfirmed that the observed positive EB originated from the sample. These results together revealed two important characteristics of the antiparallel coupling that (1) it can be promoted by field cooling but (2) it is only a metastable state.

To characterize this metastable interfacial coupling, we further studied the time dependence by thermoremanent magnetization (TRM) measurement,  $M_{TRM}(t)$ , in a total time scale of  $1.2 \times 10^{-4}$  s. For the measurements, the samples were initially cooled in positive  $H_{cool}$  ( $= 0.5, 1, 2, 3, 5, 10$  kOe) from 380 K to 300 K. After the temperature was stabilized at 300 K, with a fixed waiting time,  $t_W = 200$  s,  $H_{cool}$  was reduced to zero and the magnetization was recorded at

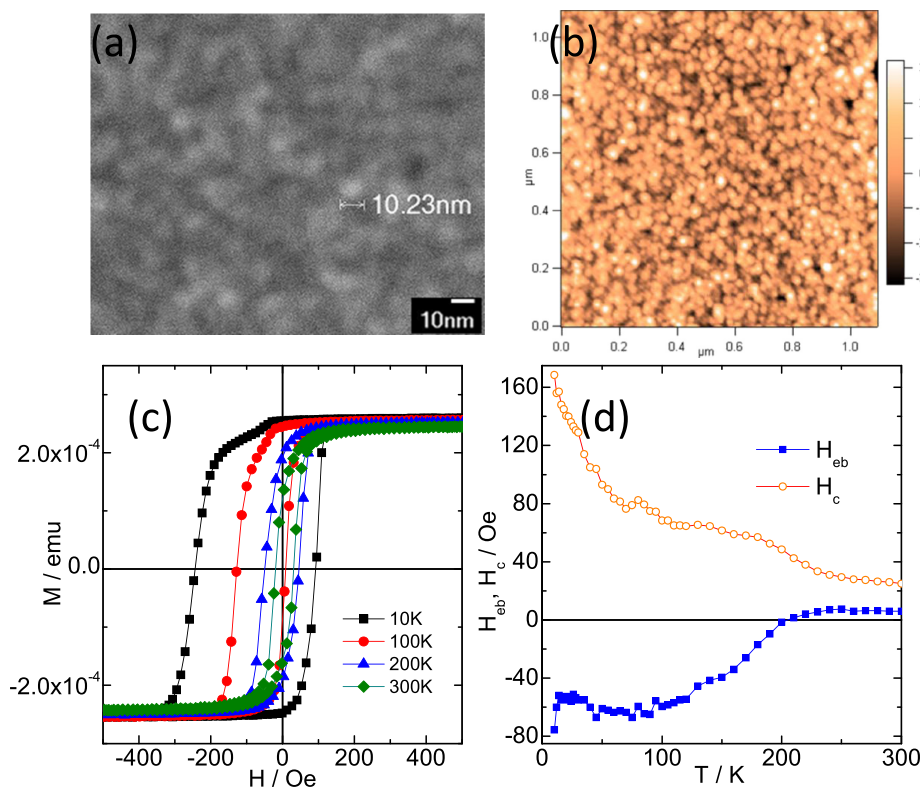


FIG. 1. SEM (a) and AFM (b) images of the Co-oxide NP film. (c) Hysteresis loops of Fe/Co-oxide bilayers measured at selective temperatures upon field cooling. (d) Temperature dependence of the coercivity,  $H_c$ , and the exchange bias,  $H_{eb}$ .

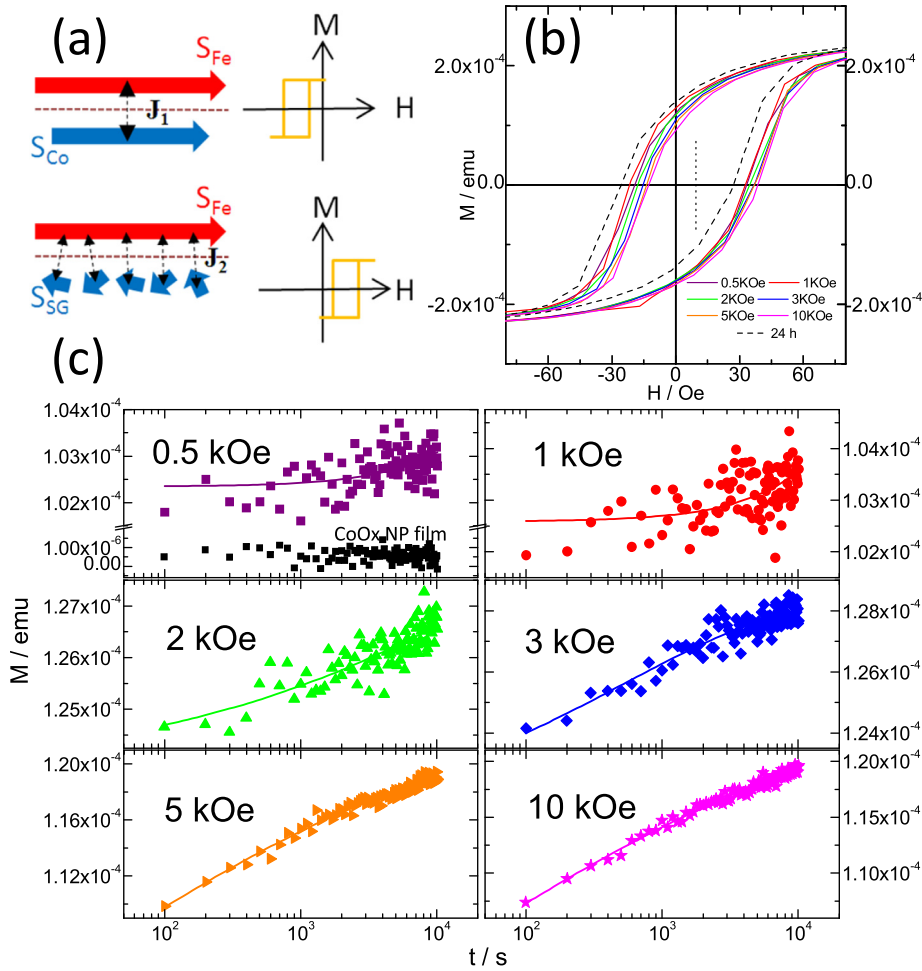


FIG. 2. (a) Schematic illustration of the effective interface coupling that leads to negative or positive EB, i.e., parallel coupling ( $J_1 > 0$ ) of  $S_{Fe}$  and  $S_{Co}$  at  $T < 200$  K, and antiparallel coupling ( $J_2 < 0$ ) of  $S_{Fe}$  and  $S_{SG}$  at  $T > 200$  K. (b) Field cooling dependence of hysteresis loops at 300 K. (c) Cooling field dependence of the relaxation behavior,  $M_{TRM}(t)$ , measured at 300 K. Sample was cooled selectively under different fields, i.e., 0.5, 1, 2, 3, 5, 10 kOe. The curves are fitted by stretched exponential function (Eq. (1)) with fitting parameters listed in Table I.

300 K in zero field as a function of time. Figure 2(c) showed the relaxation curve at each  $H_{cool}$ . The magnetization increases with time for all cooling fields. This increase, or "upward" relaxation phenomenon, is inconsistent with the general expectation that the magnetization decrease with increasing time when measured in zero applied field. However, these results are consistent with an initial magnetization component pointing against the direction of  $H_{cool}$  upon field cooling which then diminishes on aging with time. This magnetization is also not due to unoxidized Co as the samples were annealed in a very O-rich environment. To further disprove this possibility, we measured a pure Co-oxide NP film and found no ferromagnetic response (hysteresis) or magnetization relaxation. Therefore, we attribute this behavior to the surface SG magnetization,  $M_{SG}$ , of the NPs<sup>26</sup> originating from the disordered AF phase. The effect of this SG component is more significant in NPs than in continuous films<sup>18,19</sup> due to the local asymmetry of the NPs (reduced size, irregular shape, possible defects, etc). Each NP has a certain SG magnetization but they are disordered across the whole NP-film for temperatures greater than the glass transition temperature,  $T_{SG}$ . In our experiments,  $H_{cool}$  aligns the magnetic moments of FM (Fe) along the direction of the cooling field. When  $H_{cool}$  is removed, the direction of the FM magnetization,  $M_{FM}$ , remains unchanged due to the large energy barriers and associated large relaxation time. The antiparallel interface coupling between FM/SG switches the magnetization,  $M_{SG}$ , of the SG to a direction opposite to that

of the cooling field, i.e., the effective FM/SG coupling is antiferromagnetic ( $J_2 < 0$ ). This antiferromagnetic coupling simultaneously gives rise to both positive EB and the upward relaxation. When the cooling field is turned off,  $M_{SG}$  relaxes from the  $-H_{cool}$  direction to random orientations arising from thermal activation. Therefore, the magnetization of the system relaxes (increases) from  $M_{FM}-M_{SG}$  to  $M_{FM}$ . We further interpret the data by a stretched exponential function<sup>13</sup>

$$M_{TRM}(t) = M_{FM}^0 - M_{SG}^0 \exp[-(t/\tau)^{1-n}], \quad (1)$$

where  $M_{FM}^0$  and  $M_{SG}^0$  are time-independent, initial values for the FM and SG components, respectively, that are responsible for the observed relaxation behavior. The parameter  $n$  and the time constant  $\tau$  describe the relaxation rate of the SG component. The aging effect shows clear dependence with

TABLE I. Summary of fitting parameters of the relaxation curve, using Eq. (1).

| $H_{cool}$ (Oe) | $M_{FM}^0$ (emu)     | $M_{SG}^0$ (emu)     | $\tau$ (s) | $n$   |
|-----------------|----------------------|----------------------|------------|-------|
| 0.5 k           | $1.1 \times 10^{-4}$ | $7.7 \times 10^{-6}$ | 100 789    | 0.007 |
| 1 k             | $1.1 \times 10^{-4}$ | $7.4 \times 10^{-6}$ | 75 957     | 0.03  |
| 2 k             | $1.3 \times 10^{-4}$ | $6.3 \times 10^{-6}$ | 55 312     | 0.72  |
| 3 k             | $1.3 \times 10^{-4}$ | $7.3 \times 10^{-6}$ | 522        | 0.62  |
| 5 k             | $1.2 \times 10^{-4}$ | $5.0 \times 10^{-5}$ | 15         | 0.84  |
| 10 k            | $1.2 \times 10^{-4}$ | $6.0 \times 10^{-5}$ | 20         | 0.85  |



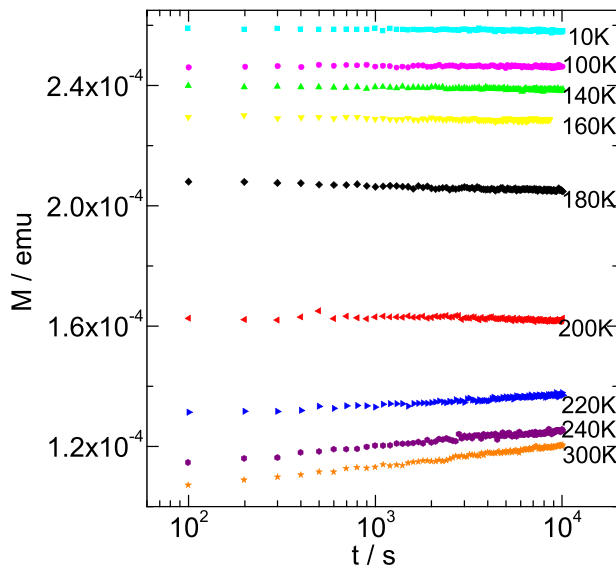


FIG. 3. Relaxation behavior,  $M_{\text{TRM}}(t)$ , of Fe/Co-oxide measured at various temperatures from 10 to 300 K. Upward relaxation is only observed for  $T > 200$  K, where the antiparallel coupling ( $J_2 < 0$ ) dominates.

the magnitude of the cooling field; stronger  $H_{\text{cool}}$  results in more significant relaxation behavior. The fitting parameters of the relaxation curves are summarized in Table I. In general,  $M_{\text{FM}}^0$  is large ( $\sim 1 \times 10^{-4}$  emu) and almost unchanged;  $M_{\text{SG}}^0$  increases with  $H_{\text{cool}}$  and  $\tau$  decreases with  $H_{\text{cool}}$ . Weak relaxation and small  $M_{\text{SG}}^0$  ( $\sim 10^{-6}$  emu) were found for small  $H_{\text{cool}}$  ( $=0.5, 1$  kOe) that can hardly be modeled by the exponential function. On the other hand, much greater  $M_{\text{SG}}^0$ , as large as  $6.0 \times 10^{-5}$  emu, is activated at  $H_{\text{cool}} = 10$  kOe. Thus, larger cooling field can effectively activate more FM/SG pairs at the interface, resulting in greater  $M_{\text{SG}}^0$  and more significant relaxation (smaller  $\tau$ ). For comparison, similar TRM measurement was also performed on pure Co-oxide NP film, Fig. 2(c). Negligibly small magnetization ( $< 10^{-6}$  emu) with almost no time dependence was observed. This indicates that without the FM/SG coupling, the external field can play no role on the SG magnetization. Finally, we measured relaxation curves at different temperatures from 10 K to 300 K upon field cooling from 380 K, using  $H_{\text{cool}} = 10$  kOe and  $t_{\text{W}} = 200$  s (Fig. 3). Upward relaxation was only observed for  $T > 200$  K, confirming that the positive EB is correlated to the surface SG behaviors. Below 200 K, normal downward relaxation was found and the time dependence is not substantial. For a complete discussion, we note that in some carefully made planar films with large

uncompensated AF magnetization,<sup>6,27,28</sup> a random AF anisotropy can also lead to a sudden change in the EB sign but below the  $T_{\text{B}}$ . A vertical shift in the hysteresis loops was observed simultaneously as a signature of the uncompensated magnetization.<sup>27,28</sup> In our particle films, the EB sign changed right above the  $T_{\text{B}}$  where the AF phase already loses its magnetic order. No signature for the AF magnetization has been observed and the strong relaxation behaviors confirmed the correlation of EB with the time-dependent SG magnetization.

Earlier work has indicated that the superexchange effect might be responsible for the positive EB observed in Co/CoO bilayers.<sup>18</sup> Here, we carefully extend such interpretation and propose a model to explain the antiparallel coupling and the magnetization relaxation based on the interfacial superexchange interaction.<sup>21</sup> Since the Co-oxide NP film was obtained from  $\text{O}_2$  annealing of Co NPs, it is expected that large areas of the surface are oxygen terminated instead of metal (Co) terminated, which gives rise to surface oxygen dangling bonds.<sup>18,25,29</sup> After the Fe layer deposition, part of the interfacial Co spins may couple with Fe spins via superexchange mechanism mediated by the oxygen atom at the interface (Fig. 4(a)). Because Fe was deposited in a vacuum chamber, with an O-deficient environment, the Fe valence state is primarily  $\text{Fe}^{2+}$  in the Fe-O-Co couple. The Co valence state is primarily  $\text{Co}^{3+}$  as confirmed by XPS measurements.<sup>25</sup> Figure 4(b) is a schematic illustration of such a  $\text{Fe}^{2+}\text{-O-Co}^{3+}$  superexchange couple. Localized electrons in Fe and Co remain in their respective orbitals and transmit spin information via the O-bridge.<sup>30</sup> Antiferromagnetic superexchange coupling arises from the mediation of oxygen  $p$  electrons according to the so-called Goodenough-Kanamori-Anderson rules.<sup>31-33</sup> In certain localized O-rich area, small numbers of  $\text{Fe}^{3+}\text{-O-Co}^{3+}$  superexchange couples with higher Fe valence state ( $\text{Fe}^{3+}$ ) may also exist; however, the nature of such coupling is still antiferromagnetic<sup>34</sup> and thus will not affect our conclusion. These Fe-O-Co couples further lead to antiparallel configuration of the FM and SG magnetization upon field cooling. Once the cooling field is cut off, each local SG magnetization relaxes to a random orientation and reduces the total  $M_{\text{SG}}$  finally to zero. It is worth noting that recently in the Fe/Fe-oxide NP system,<sup>17</sup> similar positive EB was also reported with an O-deficient interface at  $T > T_{\text{SG}}$ . Their results can also be explained within our model by considering either  $\text{Fe}^{2+}\text{-O-Fe}^{2+}$  (similar to  $\text{Fe}^{2+}\text{-O-Co}^{3+}$  couple) or  $\text{Fe}^{3+}\text{-O-Fe}^{3+}$  superexchange couple which are both antiferromagnetic.<sup>34,35</sup>

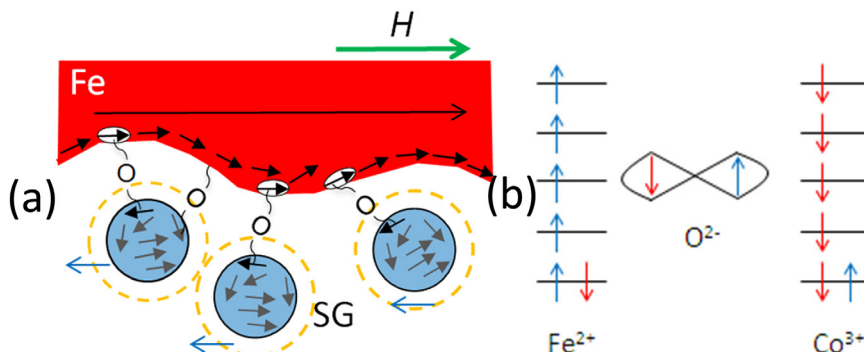


FIG. 4. Schematic illustration of (a) the antiparallel coupled  $M_{\text{FM}}$  and  $M_{\text{SG}}$  due to interface superexchange coupling and (b) antiferromagnetic superexchange interaction between  $\text{Fe}^{2+}\text{-O-Co}^{3+}$  couple.

Finally, we have noticed that for Fe/Fe-oxide systems,<sup>17</sup> at  $T < T_{SG}$ , the frozen SG gives rise to a negative EB which increases rapidly upon decreasing temperature. In our Fe/Co-oxide system, the direct exchange coupling between Fe and ordered CoO at  $T < 200$  K dominates the EB and shields the low temperature effects from the frozen SG. However, in the  $H_{eb}(T)$  curve (Fig. 1(d)), we also see a rapid increase of the EB upon temperature decrease at  $T < 15$  K, which may indicate the freezing of SG in the Fe/Co-oxide system. If the surface SG originates from  $Co_3O_4$ ,<sup>36</sup> that is known to give rise to SG behaviors below its Neel temperature,  $\sim 40$  K,<sup>37</sup> an effective  $Co_3O_4$  NP size can be then estimated to be  $\sim 5$  nm according to the finite-size effect,<sup>38</sup> which equals to approximately half of the mean diameter of the as-fabricated Co NPs.

In summary, in the hybrid Fe-film/Co-oxide NP systems, we have shown that the relaxation behavior of a spin-glass magnetization is responsible for the unconventional positive EB effect. This is due to the indirect superexchange coupling across the FM/SG interface, where Fe moments are coupled antiparallel with the spin-glass in the Co-oxides. Such SG moments do not themselves respond to the external field; however, they can show strong cooling field dependence mediated by the FM/SG coupling. Our proposed scenario of the interface also provides insight to the positive exchange bias and related properties in other metal/metal-oxide EB systems.

This work was supported by NSF/DMR 1063489. XPS surface analysis was done at NESAC/BIO under support by NIBIB Grant EB-002027. We thank Dr. Y.-C. Lee and Dr. Gerry Hammer for helpful discussions.

<sup>1</sup>W. H. Meiklejohn and C. P. Bean, *Phys. Rev.* **105**, 904 (1957).

<sup>2</sup>J. Nogues and I. K. Schuller, *J. Magn. Magn. Mater.* **192**, 203 (1999); A. E. Berkowitz and K. Takano, *ibid.* **200**, 552 (1999); R. L. Stamps, *J. Phys. D* **33**, R247 (2000); M. Kiwi, *J. Magn. Magn. Mater.* **234**, 584 (2001).

<sup>3</sup>P. Blomqvist, K. M. Krishnan, and D. E. McCready, *J. Appl. Phys.* **95**, 8019 (2004).

<sup>4</sup>S. Bruck, G. Schutz, E. Goering, X. Ji, and K. M. Krishnan, *Phys. Rev. Lett.* **101**, 126402 (2008).

<sup>5</sup>G. Srajer, L. H. Lewis, S. D. Bader, A. J. Epstein, C. S. Fadley, E. E. Fullerton, A. Hoffmann, J. B. Kortright, K. M. Krishnan, S. A. Majetich, T. S. Rahman, C. A. Ross, M. B. Salamon, I. K. Schuller, T. C. Schulthess, and J. Z. Sun, *J. Magn. Magn. Mater.* **307**, 1 (2006).

<sup>6</sup>K. O'Grady, L. E. Fernandez-Outon, and G. Vallejo-Fernandez, *J. Magn. Magn. Mater.* **322**, 883 (2010).

<sup>7</sup>T. Wen and K. M. Krishnan, *J. Phys. D: Appl. Phys.* **44**, 393001 (2011).

<sup>8</sup>J. Nogues, J. Sort, V. Langlais, V. Skumryev, S. Surinach, J. S. Munoz, and M. D. Baro, *Phys. Rep.* **422**, 65 (2005).

<sup>9</sup>R. H. Kodama, A. E. Berkowitz, E. J. McNiff, and S. Foner, *Phys. Rev. Lett.* **77**, 394 (1996).

<sup>10</sup>B. Martnez, X. Obradors, Ll. Balcells, A. Rouanet, and C. Monty, *Phys. Rev. Lett.* **80**, 181 (1998).

<sup>11</sup>H. Wang, T. Zhu, K. Zhao, W. N. Wang, C. S. Wang, Y. J. Wang, and W. S. Zhan, *Phys. Rev. B* **70**, 092409 (2004).

<sup>12</sup>T. Mousavand, T. Naka, K. Sato, S. Ohara, M. Umetsu, S. Takami, T. Nakane, A. Matsushita, and T. Adschiri, *Phys. Rev. B* **79**, 144411 (2009).

<sup>13</sup>C.-P. Chen, L. He, Y. Leng, and X. Li, *J. Appl. Phys.* **105**, 123923 (2009).

<sup>14</sup>V. Baltz, G. Gaudin, P. Somani, and B. Dieny, *Appl. Phys. Lett.* **96**, 262505 (2010).

<sup>15</sup>M. Ali, P. Adie, C. H. Marrows, D. Greig, B. J. Hickey, and R. L. Stamps, *Nat. Mater.* **6**, 70 (2007).

<sup>16</sup>Y.-C. Lee, A. B. Pakhomov, and K. M. Krishnan, *J. Appl. Phys.* **107**, 09E124 (2010).

<sup>17</sup>W. Wang, F. Takano, M. Takenaka, H. Akinaga, and H. Ofuchi, *J. Appl. Phys.* **103**, 093914 (2008).

<sup>18</sup>F. Radu, M. Etzkorn, R. Siebrecht, T. Schmitte, K. Westerholt, and H. Zabel, *Phys. Rev. B* **67**, 134409 (2003).

<sup>19</sup>C. Prados, E. Pina, A. Hernando, and A. Montone, *J. Phys.: Condens. Matter* **14**, 10063 (2002).

<sup>20</sup>T. Gredig, I. N. Krivorotov, P. Eames, and E. D. Dahlberg, *Appl. Phys. Lett.* **81**, 1270 (2002).

<sup>21</sup>P. W. Anderson, *Phys. Rev.* **79**, 350 (1950).

<sup>22</sup>V. F. Puentes, K. M. Krishnan, and P. A. Alivisatos, *Science* **291**, 2115 (2001).

<sup>23</sup>Y. Bao, M. Beerman, A. B. Pakhomov, and K. M. Krishnan, *J. Phys. Chem. B* **109**, 7220 (2005).

<sup>24</sup>T. L. Wen and S. A. Majetich, *ACS Nano* **22**, 8868 (2011).

<sup>25</sup>See supplementary material at <http://dx.doi.org/10.1063/1.4754610> for XPS measurements.

<sup>26</sup>L. He, *J. Appl. Phys.* **109**, 123915 (2011).

<sup>27</sup>M. Cheon, Z. Liu, and D. Lederman, *Appl. Phys. Lett.* **90**, 012511 (2007).

<sup>28</sup>M. Cheon, Z. Liu, and D. Lederman, *J. Appl. Phys.* **101**, 09E503 (2007).

<sup>29</sup>M. De Santis, A. Buchsbaum, P. Varga, and M. Schmid, *Phys. Rev. B* **84**, 125430 (2011).

<sup>30</sup>L. He and L. Guo, *Appl. Phys. Lett.* **97**, 182509 (2010).

<sup>31</sup>J. Kanamori, *J. Phys. Chem. Solid* **10**, 87 (1959).

<sup>32</sup>P. W. Anderson, in *Magnetism*, edited by G. T. Rado and H. Suhl (Academic, New York, 1963), Chap. 2, pp. 25–83.

<sup>33</sup>J. B. Goodenough, *Magnetism and the Chemical Bond* (Interscience, New York, 1963).

<sup>34</sup>X. Luo, W. Xing, Z. Li, G. Wu, and X. Chen, *Phys. Rev. B* **75**, 054413 (2007).

<sup>35</sup>M.-H. Phan, T.-L. Phan, T.-N. Huynh, S.-C. Yu, J. R. Rhee, N. V. Khien, and N. X. Phuc, *J. Appl. Phys.* **95**, 7531 (2004).

<sup>36</sup>P. Dutta, M. S. Seehra, S. Thota, and J. Kumar, *J. Phys.: Condens. Matter* **20**, 015218 (2008).

<sup>37</sup>S. Gangopadhyay, G. C. Hadjipanayis, C. M. Sorensen, and K. J. Klambunde, *J. Appl. Phys.* **73**, 6964 (1993).

<sup>38</sup>L. He, C.-P. Chen, N. Wang, W. Zhou, and L. Guo, *J. Appl. Phys.* **102**, 103911 (2007).